Contribution from the Department of Chemistry and Biochemistry, University of Colorado, Boulder, Colorado 80309

Structure and Bonding in Bis(quinone) Complexes of Ruthenium. Synthesis and Characterization of the $Ru(PPh_3)_2(SQ)_2$ (SQ = 3,5-Di-*tert*-butylsemiquinone, Tetrachloro-1,2-semiquinone) Series

Samaresh Bhattacharya and Cortlandt G. Pierpont*

Received July 31, 1990

Questions concerning charge distribution in the neutral bis(quinone) complexes of ruthenium have prompted investigation of members of the $Ru(PPh_3)_2(SQ)_2$ (SQ = 3,5-di-*tert*-butylsemiquinone (DBSQ), tetrachloro-1,2-semiquinone (Cl_4SQ)) series. $Ru(PPh_3)_2(DBSQ)Cl_2$ has been synthesized and characterized as a precursor. Crystals of $Ru(PPh_3)_2(DBSQ)Cl_2$ form in the monoclinic space group $P2_1/c$ with $Z = 4$ in a unit cell of dimensions $a = 16.544$ (3) Å, $b = 12.217$ (2) Å, $c = 22.535$ (5) Å, and $\beta = 100.65$ (3)°. Structural features of the quinone ligand indicate that it is a semiquinone and that the complex contains Ru(III). The diamagnetism of the complex results from strong antiferromagnetic coupling between the paramagnetic metal and the coordinated radical. Treatment of the complex with a second catecholate ligand leads to displacement of the chloro ligands with formation of the bis(quinone) product. Complexes containing combinations of 3,5-di-*tert*-butylcatechol and tetrachlorocatechol have been studied, and $Ru(PPh_3)_2(Cl_4SQ)_2$ has been characterized crystallographically as a dichloromethane solvate. Crystals form in the triclinic space group $P\bar{1}$ with $Z = 2$ in a unit cell of dimensions $a = 12.586$ (2) Å, $b = 12.893$ (2) Å, $c = 17.351$ (2) Å, $\alpha = 87.156$ (13)°, $\beta = 82.806$ (11)°, and $\gamma = 66.285$ (12)°. Structural features of the quinone ligands agree with values expected for semiquinones, pointing to the $Ru(PPh_3)_2(Cl_4SQ)_2$ charge distribution in the solid state. Similarities in the infrared spectra of $Ru(PPh_3)_2(DBSQ)Cl_2$ and $Ru(PPh_3)_2(DBSQ)_2$ indicate a similar charge distribution for the $(DBSQ)_2$ complex. Electrochemical characterization has shown that each of the bis(quinone) complexes undergoes two oxidations and two reductions with potentials for members of each four-membered series shifted progressively in a negative direction for $Ru(PPh_3)_2(Cl_4SQ)_2$, $Ru(PPh_3)_2(DBSQ)(Cl_4SQ)$, and $Ru(PPh_3)_2(DBSQ)_2$, respectively. Values of these potentials are quite similar to corresponding couples of the related bipyridine complexes, $Ru(bpy)(SQ)_2$. This result, with similarities in the electronic spectra for the two classes of complexes, has been interpreted to indicate that the bipyridine and triphenylphosphine complexes have similar charge distributions in solution and that the redox-active electronic levels are ligand-delocalized molecular orbitals.

Introduction

Early structure determinations on complexes containing semiquinone and catecholate ligands indicated that the C–O bond lengths of quinone ligands are particularly sensitive to ligand charge and may be used to provide information on charge distribution between ligand and metal.[1] In particular, C–O bond lengths of 1.34, 1.29, and 1.23 Å have been found from a large number of studies to be characteristic of coordinated catecholate, semiquinone, and *o*-benzoquinone electronic forms of quinone ligands. Spectroscopic and magnetic properties are often also available to confirm the assignment of charge. Electronic delocalization between ligand and metal appears to be less important for this class of ligands than for related complexes of the 1,2-dithiolenes or 1,2-diimines.[2] Structural results obtained on neutral bis(quinone) complexes of ruthenium seemed to show a break in this pattern. Ligand C–O bond lengths of 1.321 (5) Å were found for both $Ru(bpy)(Q)_2$ and *trans*-$Ru(4\text{-}t\text{-}Bupy)_2(DBQ)_2$, intermediate between semiquinone and catecholate values but consistent with a delocalized $Ru^{III}(N\text{-}N)(SQ)(Cat)$ species.[3,4] Spectroscopic characterization on these and related complexes failed to provide definitive information on charge distribution; however, the diamagnetism of the complexes suggested a strong metal orbital contribution to the ground state.[5]

Equivalence of the quinone ligands may arise from strong interligand electronic coupling that may not include a metal orbital contribution.[6] To investigate this possibility, we have sought to prepare complexes with electronically different quinone ligands in an attempt to localize interligand charge transfer. The tetrachloroquinone and di-*tert*-butylquinone ligands have corresponding redox potentials that differ by approximately 0.5 V. It might be anticipated that within a mixed-ligand complex related to the $Ru^{III}(N\text{-}N)(SQ)(Cat)$ series, the tetrachloroquinone ligand with the most positive reduction potential would bond in the reduced catecholate form, $Ru(N\text{-}N)(DBSQ)(Cl_4Cat)$. As a synthon to mixed-ligand complexes, $Ru(PPh_3)_2(DBSQ)Cl_2$ has been prepared to yield a series containing triphenylphosphine counter ligands rather than nitrogen donors. The properties of this complex and the bis(quinone) complexes formed from this precursor are described below.

Experimental Section

Materials. $Ru(PPh_3)_3Cl_2$ was prepared by a published procedure.[7] 3,5-Di-*tert*-butylcatechol (H_2DBCat) and 3,5-di-*tert*-butyl-1,2-benzoquinone (DBBQ) were purchased from Aldrich and used as received. Tetrachlorocatechol (H_2Cl_4Cat) was prepared by a published procedure and sublimed before use.[8]

Preparation of Complexes. $Ru(PPh_3)_2(DBSQ)Cl_2$. Degassed dichloromethane (50 mL) was added to a mixture of $Ru(PPh_3)_3Cl_2$ (1.0 g, 1.04 mmol) and DBBQ (230 mg, 1.04 mmol) under N_2. Within minutes the color of the solution became blue. The mixture was stirred for 5 h, hexane was layered over the solution to induce crystallization, and a stream of N_2 was passed over the solution to cause slow evaporation. $Ru(PPh_3)_2(DBSQ)Cl_2$ (750 mg) was obtained as a dark blue crystalline solid in 78% yield. The complex was characterized spectroscopically and crystallographically.

$Ru(PPh_3)_2(DBSQ)(Cl_4SQ)$ and $Ru(PPh_3)_2(Cl_4SQ)_2$. Degassed dichloromethane was added to a mixture of $Ru(PPh_3)_2(DBSQ)Cl_2$ (478 mg, 0.52 mmol) and H_2Cl_4Cat (160 mg, 0.65 mmol) under N_2. Triethylamine (0.6 mL, 4.31 mmol) was then added, and the solution was stirred for 20 h. The solvent was then evaporated under reduced pressure; the solid residue was dissolved in benzene, and the mixture was filtered to remove insoluble material. The benzene filtrate was then chromatographed on an alumina column using benzene as the eluant. A pale yellow band appeared first and was rejected. The next two bands, blue-green and purple, were collected separately and evaporated slowly to give crystalline solids. The purple fraction gave $Ru(PPh_3)_2(DBSQ)(Cl_4SQ)$ (250 mg) in 44% yield; the blue-green fraction gave

(1) Pierpont, C. G.; Buchanan, R. M. *Coord. Chem. Rev.* **1981**, *38*, 44.
(2) McCleverty, J. A. *Prog. Inorg. Chem.* **1968**, *10*, 49.
(3) Boone, S. R.; Pierpont, C. G. *Polyhedron* **1990**, *9*, 2267.
(4) (a) Haga, M.; Dodsworth, E. S.; Lever, A. B. P.; Boone, S. R.; Pierpont, C. G. *J. Am. Chem. Soc.* **1986**, *108*, 7321. (b) Boone, S. R.; Pierpont, C. G. *Inorg. Chem.* **1987**, *26*, 1769.
(5) Lever, A. B. P.; Auburn, P. R.; Dodsworth, E. S.; Haga, M.; Liu, W.; Melnik, M.; Nevin, W. A. *J. Am. Chem. Soc.* **1988**, *110*, 8076.
(6) Vogler, A.; Kunkely, H. *Comments Inorg. Chem.* **1990**, *9*, 201.
(7) Stephenson, T. A.; Wilkinson, G. *J. Inorg. Nucl. Chem.* **1966**, *28*, 945.
(8) (a) Jackson, L. C.; MacLaurin, R. D. *J. Am. Chem. Soc.* **1907**, *37*, 11. (b) Abbreviations: BQ, SQ, and Cat have been used to refer to benzoquinone, semiquinone, and catecholate forms of the quinone ligands, Q has been used to refer to quinone ligands of unspecified charge, and DB and Cl_4 have been used as prefixes for the 3,5-di-*tert*-butyl- and tetrachloro-substituted quinone ligands.

0020-1669/91/1330-1511$02.50/0

Table I. Crystallographic Data for $Ru(PPh_3)_2(DBSQ)Cl_2$ and $Ru(PPh_3)_2(Cl_4SQ)_2 \cdot CH_2Cl_2$[a]

	$Ru(PPh_3)_2(DBSQ)Cl_2$	$Ru(PPh_3)_2(Cl_4SQ)_2 \cdot CH_2Cl_2$
mol wt	916.8	1202.3
color	blue	blue-green
cryst system	monoclinic	triclinic
space group	$P2_1/c$	$P\bar{1}$
a, Å	16.544 (3)	12.586 (2)
b, Å	12.217 (2)	12.893 (2)
c, Å	22.535 (5)	17.351 (2)
α, deg	90.00	87.156 (13)
β, deg	100.65 (3)	82.806 (11)
γ, deg	90.00	66.285 (12)
V, Å^3	4476.3 (15)	2557.7 (7)
Z	4	2
D_{calcd}, g cm^{-3}	1.360	1.561
D_{exptl}, g cm^{-3}	1.359	1.560
μ, cm^{-1}	5.71	9.31
T_{max}, T_{min}	0.884, 0.837	0.715, 0.788
R, R_w	0.037, 0.044	0.053, 0.073
GOF	1.25	1.71

[a] Radiation, Mo Kα (0.71073 Å); temperature, 294–297 K.

$Ru(PPh_3)_2(Cl_4SQ)_2$ (110 mg) in 19% yield. Both complexes were characterized spectroscopically; $Ru(PPh_3)_2(Cl_4SQ)_2$ was characterized crystallographically.

$Ru(PPh_3)_2(DBSQ)_2$. Procedure 1. $Ru(PPh_3)_3Cl_2$ (500 mg, 0.52 mmol) was added to a solution containing NaOH (90 mg, 2.25 mmol) and H_2DBCat (250 mg, 1.13 mmol) dissolved in 40 mL of ethanol. The mixture was stirred for 6 h in air and filtered, and the filtrate was evaporated. The solid residue was dissolved in benzene, the mixture was filtered, and the filtrate was chromatographed on an alumina column using benzene as the eluant. The major blue-green fraction was collected and evaporated to give dark crystals of $Ru(PPh_3)_2(DBSQ)_2$ (350 mg) in 63% yield.

Procedure 2. Degassed dichloromethane (50 mL) was added to a mixture of $Ru(PPh_3)_2(DBSQ)Cl_2$ (700 mg, 0.76 mmol) and H_2DBCat (190 mg, 0.86 mmol). Triethylamine (0.8 mL, 5.75 mmol) was then added, and the solution was stirred for 4 h. The solvent was evaporated, the solid residue was dissolved in benzene, and the solution was filtered and chromatographed as above. $Ru(PPh_3)_2(DBSQ)_2$ (600 mg) was obtained as a dark blue-green crystalline solid in 74% yield.

Physical Measurements. Electronic spectra were recorded on a Perkin-Elmer Lambda 9 spectrophotometer. Infrared spectra were obtained on an IBM IR/30 FTIR spectrometer with samples prepared as KBr pellets. ^1H NMR spectra were recorded on a Varian VXR 300S spectrometer. Cyclic voltammograms were obtained with a Cypress CYSY-1 computer-controlled electroanalysis system in CH_2Cl_2 and CH_3CN solutions. A platinum-disk working electrode and a platinum-wire counter electrode were used. A Ag/Ag^+ reference electrode was used that consisted of a CH_3CN solution of $AgPF_6$ in contact with a silver wire placed in glass tubing with a Vycor frit at one end to allow ion transport. Tetrabutylammonium perchlorate (TBAP) was used as the supporting electrolyte, and the ferrocene/ferrocenium couple was used as an internal standard.

Crystallographic Structure Determinations. $Ru(PPh_3)_2(DBSQ)Cl_2$. Dark blue prismatic crystals of $Ru(PPh_3)_2(DBSQ)Cl_2$ were obtained by slow evaporation of a CH_2Cl_2/hexane solution of the complex. Axial photographs indicated monoclinic symmetry, and the centered settings of 25 reflections in the 2θ range between 20 and 33° gave the unit cell dimensions listed in Table I. Data were collected by θ–2θ scans within the angular range 3.0–45.0°. The Ru location was determined from a Patterson map, and the positions of other atoms of the structure were determined from the phases generated by the heavy atoms. Final cycles of least-squares refinement converged with discrepancy indices of R = 0.037 and R_w = 0.044. Final positional parameters for selected atoms of the structure are contained in Table II. Tables containing full listings of atom positions, anisotropic thermal parameters, and hydrogen atom locations are available as supplementary material.

$Ru(PPh_3)_2(Cl_4SQ)_2$. Dark blue-green crystals of $Ru(PPh_3)_2(Cl_4SQ)_2$ were obtained by slow evaporation of a CH_2Cl_2/acetone solution of the complex. Axial photographs indicated triclinic symmetry, and the centered settings of 25 reflections in the 2θ range between 24 and 36° gave the unit cell dimensions listed in Table I. Data were collected by θ–2θ scans within the angular range 3.0–45.0°. The Ru location was determined from a Patterson map, and the positions of other atoms of the structure were determined from the phases generated by the heavy atoms.

Table II. Selected Atomic Coordinates (×10^4) for $Ru(PPh_3)_2(DBSQ)Cl_2$

	x/a	y/b	z/c
Ru	2832 (1)	1370 (1)	1462 (1)
Cl1	4224 (1)	1350 (1)	1393 (1)
Cl2	2295 (1)	1793 (1)	456 (1)
P1	2764 (1)	−539 (1)	1177 (1)
P2	2895 (1)	3299 (1)	1708 (1)
O1	3165 (2)	912 (3)	2322 (1)
O2	1714 (2)	1369 (3)	1751 (1)
C1	2568 (3)	771 (4)	2615 (2)
C2	1759 (3)	1065 (4)	2311 (2)
C3	1086 (3)	1012 (4)	2632 (2)
C4	1278 (3)	623 (4)	3216 (2)
C5	2081 (3)	300 (4)	3514 (2)
C6	2721 (3)	376 (4)	3213 (2)
C7	213 (3)	1412 (5)	2373 (2)
C11	2188 (4)	−108 (6)	4164 (3)

Table III. Selected Atomic Coordinates (×10^4) for $Ru(PPh_3)_2(Cl_4SQ)_2$

	x/a	y/b	z/c
Ru	2119 (1)	3700 (1)	2448 (1)
Cl1	−2003 (2)	6575 (2)	2870 (1)
Cl2	−2838 (2)	7695 (2)	1274 (2)
Cl3	−1060 (2)	7145 (2)	−219 (1)
Cl4	1547 (2)	5486 (2)	−126 (1)
Cl5	1163 (3)	2334 (2)	5018 (1)
Cl6	−838 (3)	1474 (3)	5000 (2)
Cl7	−1624 (2)	1175 (3)	3431 (2)
Cl8	−538 (2)	1916 (3)	1871 (2)
P1	2853 (2)	4953 (2)	2930 (1)
P2	3901 (2)	2230 (2)	2009 (1)
O1	1941 (4)	4510 (4)	1437 (3)
O2	469 (4)	4953 (4)	2699 (3)
O3	1213 (5)	2809 (5)	2126 (3)
O4	1977 (5)	2911 (4)	3449 (3)
C1	865 (7)	5168 (6)	1364 (4)
C2	79 (6)	5412 (6)	2059 (4)
C3	−1078 (7)	6241 (7)	2012 (5)
C4	−1430 (7)	6741 (7)	1333 (5)
C5	−620 (7)	6501 (7)	649 (5)
C6	507 (7)	5736 (7)	672 (4)
C7	715 (7)	2527 (7)	2746 (5)
C8	1102 (7)	2595 (7)	3485 (5)
C9	635 (8)	2245 (7)	4170 (5)
C10	−194 (9)	1833 (8)	4149 (6)
C11	−576 (8)	1723 (7)	3436 (6)
C12	−132 (7)	2055 (7)	2760 (6)

A half-molecule of CH_2Cl_2 was found to be located at a general position in the unit cell, and a second was found close to the inversion center at [0,0,0]. The second CH_2Cl_2 molecule was found to be extensively disordered and was treated with atoms of fractional occupancy. Final cycles of least-squares refinement converged with discrepancy indices of R = 0.053 and R_w = 0.073. Final positional parameters for selected atoms of the structure are contained in Table III. Tables containing full listings of atom positions, anisotropic thermal parameters, and hydrogen atom locations are available as supplementary material.

Experimental Results

$Ru(PPh_3)_2(DBSQ)Cl_2$. The reaction between $Ru(PPh_3)_3Cl_2$ and DBBQ gives $Ru(PPh_3)_2(DBSQ)Cl_2$ with displacement of a triphenylphosphine ligand. The complex is diamagnetic and shows sharp *tert*-butyl proton resonances for the quinone ligand. Two sets of resonances, 1.099–1.209 and 1.509–1.828 ppm, of approximate ratio 3:1 are observed corresponding to two isomers of the complex, related by different orientations of the DBSQ ligand. With the Ru(III)–SQ charge distribution chosen for the complex, diamagnetism must result from strong antiferromagnetic coupling between the paramagnetic metal and the radical ligand. Other diamagnetic options for localized charge distribution include Ru(II)–BQ or Ru(IV)–Cat forms. Spectroscopic properties provide little information on metal charge, but structural features of the quinone ligand have proven to be consistent with the Ru(III)–SQ form. A view of the $Ru(PPh_3)_2(DBSQ)Cl_2$ molecule

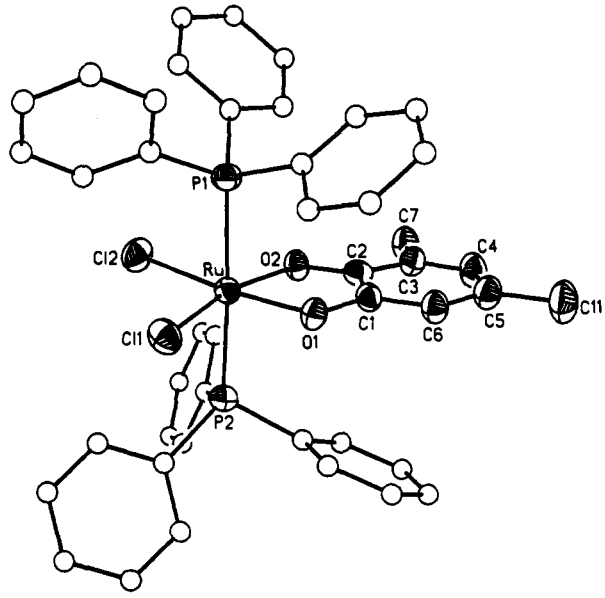

Figure 1. View of the $Ru(PPh_3)_2(DBSQ)Cl_2$ complex molecule drawn with 50% thermal ellipsoids. Methyl carbon atoms of the *tert*-butyl groups have been omitted.

Table IV. Selected Bond Distances and Angles for $Ru(PPh_3)_2(DBSQ)Cl_2$

	Distances (Å)		
Ru–O1	1.995 (3)	C2–O2	1.305 (6)
Ru–O2	2.071 (3)	C1–C2	1.432 (6)
Ru–P1	2.416 (1)	C2–C3	1.437 (7)
Ru–P2	2.419 (1)	C3–C4	1.379 (7)
Ru–Cl1	2.336 (1)	C4–C5	1.429 (7)
Ru–Cl2	2.333 (1)	C5–C6	1.363 (8)
C1–O1	1.298 (6)	C6–C1	1.409 (7)
	Angles (deg)		
Cl1–Ru–Cl2	98.1 (1)	Cl1–Ru–P1	88.3 (1)
Cl2–Ru–P1	88.0 (1)	Cl1–Ru–P2	91.4 (1)
Cl2–Ru–P2	90.0 (1)	P1–Ru–P2	177.9 (1)
Cl1–Ru–O1	87.9 (1)	Cl2–Ru–O1	173.1 (1)
P1–Ru–O1	88.8 (1)	P2–Ru–O1	93.3 (1)
Cl1–Ru–O2	165.7 (1)	Cl2–Ru–O2	95.9 (1)
P1–Ru–O2	94.7 (1)	P2–Ru–O2	86.1 (1)
O1–Ru–O2	78.2 (1)		

is shown in Figure 1, and selected bond distances and angles are given in Table IV. Phosphine ligands are trans to one another in the complex molecule. One phenyl ring bound to P2 is located below the quinone ligand in Figure 1, and it appears to be coupled with the quinone through a weak π interaction. Features of the quinone ligand are in accord with the pattern of bond lengths found for DBSQ ligands in other complexes where spectroscopic and magnetic properties provide additional information on charge distribution. The C–O bond lengths average 1.302 (6) Å, within the range of values expected for a semiquinone ligand.[1] Further, the pattern of C–C bond lengths within the quinone ring agrees with the partially localized quinone bonding structure generally observed for semiquinone ligands.[9] The C3–C4 and C5–C6 lengths of 1.379 (7) and 1.363 (8) Å are significantly shorter than other ring C–C lengths. Structural features of $Ru(PPh_3)_2(DBSQ)Cl_2$ point strongly to the Ru(III)–SQ charge distribution. The electronic spectrum of the complex in the visible region (Figure 2) consists of a band at 509 nm and a second stronger and slightly unsymmetrical band at 700 nm. The infrared spectrum of $Ru(PPh_3)_2(DBSQ)Cl_2$, shown in Figure 3, provides little insight into charge distribution, but it is useful for purposes of comparison with other related complexes. Electrochemical characterization on the complex has shown that it undergoes

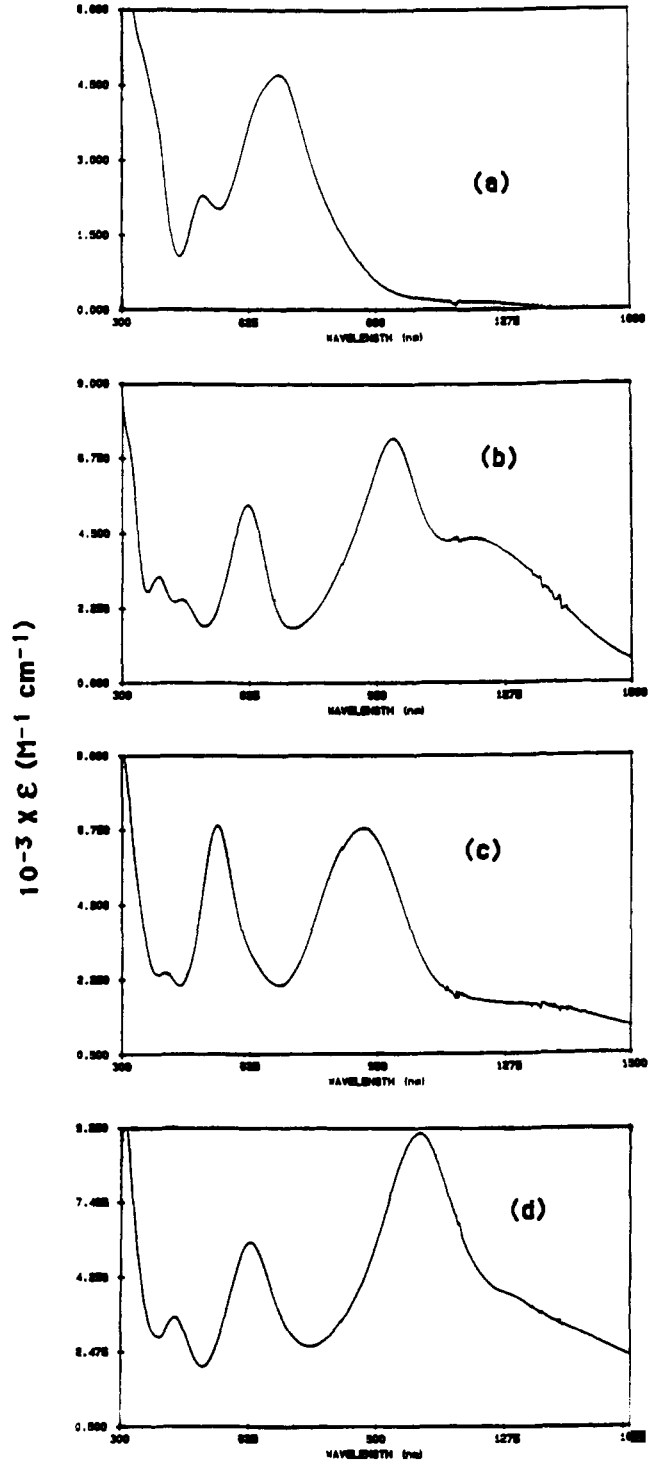

Figure 2. Visible and near-IR absorption spectra of (a) $Ru(PPh_3)_2(DBSQ)Cl_2$, (b) $Ru(PPh_3)_2(DBSQ)_2$, (c) $Ru(PPh_3)_2(DBSQ)(Cl_4SQ)$, and (d) $Ru(PPh_3)_2(Cl_4SQ)_2$. Spectra were recorded in CH_2Cl_2 solutions.

reversible reduction at −0.775 V and oxidation at 0.297 V (vs Fc/Fc^+). The reduction potential is close to potentials of the corresponding DBCat/DBSQ couples of $M(bpy)_2(DBCat)$, M = Ru and Os, and appears related to reduction of the semiquinone ligand.[10] The oxidation potential is slightly more positive than the oxidation potentials of the bipyridine complexes where metal and quinone orbital mixing appears to be significant. Orbital mixing may also contribute to the reversibility of the couple for $Ru(PPh_3)_2(DBSQ)Cl_2$, since oxidation of the semiquinone would produce benzoquinone, a process that usually leads to ligand

(9) Boone, S. R.; Purser, G. H.; Chang, H.-R.; Lowery, M. D.; Hendrickson, D. N.; Pierpont, C. G. *J. Am. Chem. Soc.* **1989**, *111*, 2292.

(10) Haga, M.; Isobe, K.; Boone, S. R.; Pierpont, C. G. *Inorg. Chem.* **1990**, *29*, 3795.

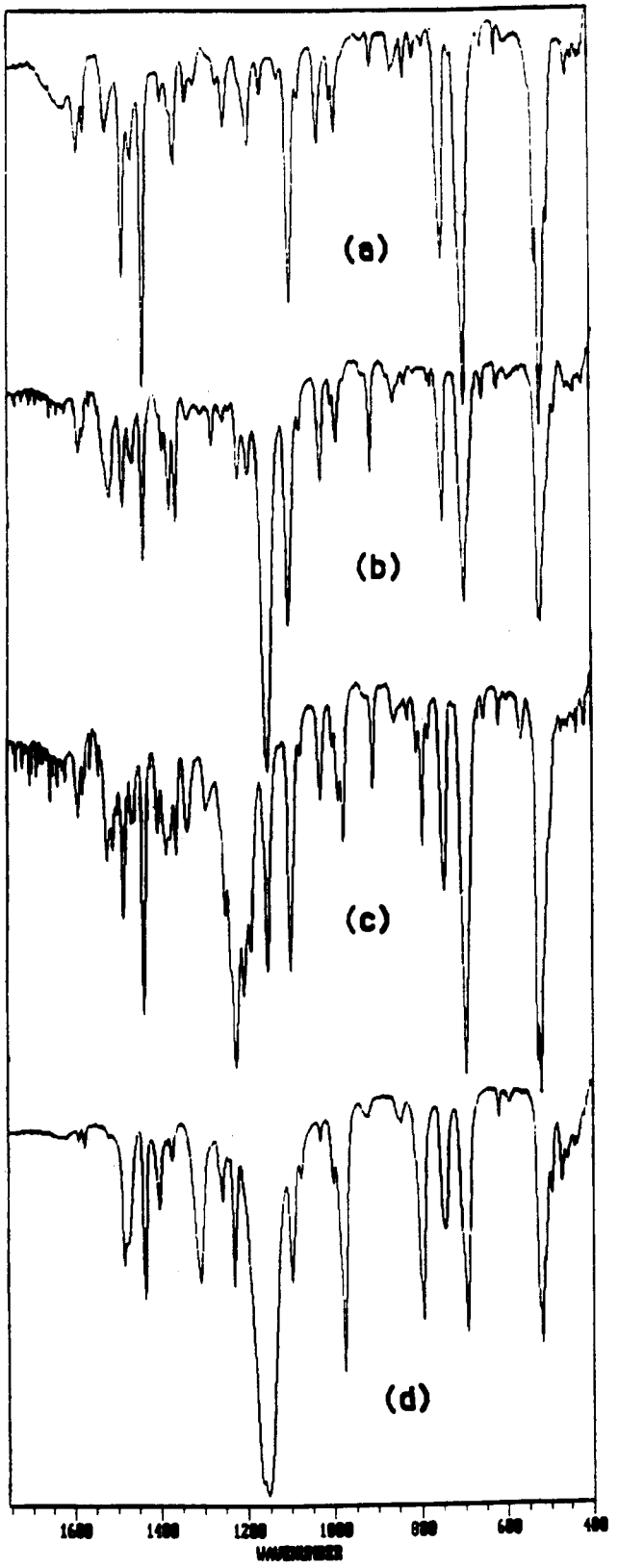

Figure 3. Infrared spectra of (a) $Ru(PPh_3)_2(DBSQ)Cl_2$, (b) $Ru(PPh_3)_2(DBSQ)_2$, (c) $Ru(PPh_3)_2(DBSQ)(Cl_4SQ)$, and (d) $Ru(PPh_3)_2(Cl_4SQ)_2$. Samples were prepared as KBr pellets.

dissociation and electrochemical irreversibility.

$Ru(PPh_3)_2(DBSQ)_2$. The bis(quinone) product $Ru(PPh_3)_2(DBSQ)_2$ can be formed either by treating $Ru(PPh_3)_2(DBSQ)Cl_2$ with DBCat or by treating $Ru(PPh_3)_3Cl_2$ with DBSQ. Several isomers are available for the complex. Three sets of *tert*-butyl resonances are observed in the ^1H NMR spectrum at 0.624–1.310, 0.764–1.353, and 1.145–1.372 ppm in a ratio of 2:1.3:1, respectively. These indicate that the complex is diamagnetic and may also indicate that the form of the complex obtained is the cis isomer. The cis disposition of the PPh_3 ligands may be stabilized by intramolecular π interactions between the phosphine phenyl rings and the rings of the quinone ligands. The electronic spectrum of $Ru(PPh_3)_2(DBSQ)_2$, shown in Figure 2, consists of weaker bands at 392 and 452 nm, bands of intermediate strength at 623 and 994 nm, and a broad band at 1200 nm. The infrared spectrum of the complex shown in Figure 3 has a number of bands in common with $Ru(PPh_3)(DBSQ)Cl_2$. The most notable difference between the spectrum of this complex and the spectrum of the dichloro complex is the appearance of an intense band at 1080 cm^{-1}. Cyclic voltammograms recorded on $Ru(PPh_3)_2(DBSQ)_2$ show the four couples, two oxidations and two reductions, listed in Table V and shown in Figure 4. The potentials of these couples are quite similar to the potentials of the redox series of Ru-

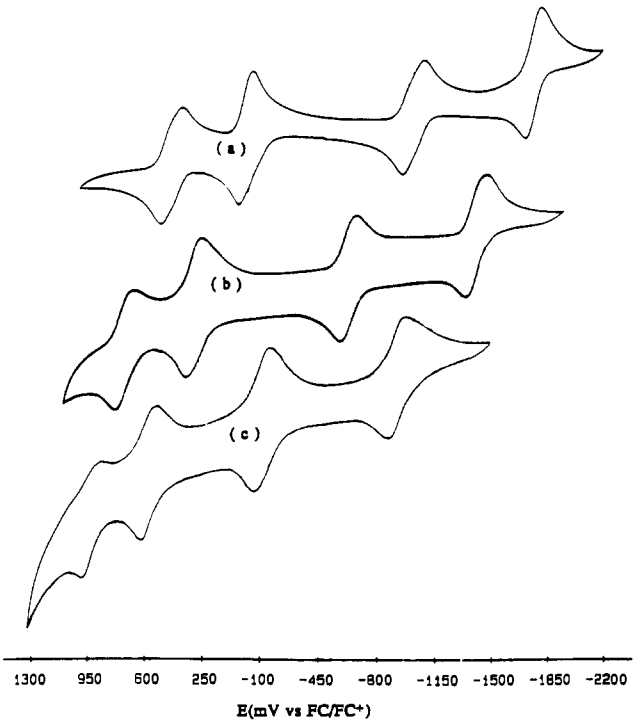

Figure 4. Cyclic voltammograms, showing the four-membered redox series of (a) $Ru(PPh_3)_2(DBSQ)_2$, (b) $Ru(PPh_3)_2(DBSQ)(Cl_4SQ)$, and (c) $Ru(PPh_3)_2(Cl_4SQ)_2$. Acetonitrile (0.1 M TBAP) was used as the solvent; scan rates were 100 mV/s.

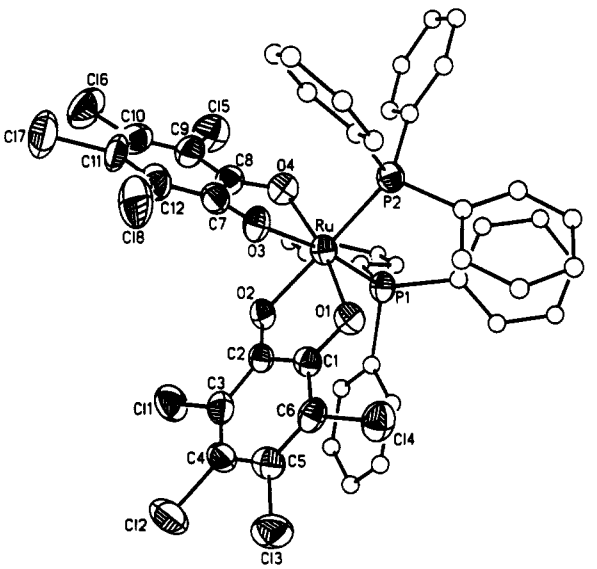

Figure 5. View of the $Ru(PPh_3)_2(Cl_4SQ)_2$ complex molecule drawn with 50% thermal ellipsoids.

Table V. Electrochemical and Electronic Spectroscopic Data for the $RuL_2(SQ)_2$ Series

complex	$E_{1/2}$, V vs Fc/Fc^+ (ΔE, mV)[a]				λ_{max}, nm (ϵ, M^{-1} cm^{-1})[c]
	oxdn II	oxdn I	redn I	redn II	
$Ru(PPh_3)_2(DBSQ)_2$	0.407 (120)	−0.045 (72)	−1.052 (118)	−1.791 (92)	392 (3200), 452 (2500), 623 (5300), 994 (7400), 1200 (4300)
$Ru(bpy)(DBSQ)_2$[b,c]	0.58	−0.11	−1.13	−1.84	375 (5700), 505 (3100), 605 (11 600), 955 (12 100), 1175 (6050)
$Ru(PPh_3)_2(DBSQ)(Cl_4SQ)$	0.690 (95)	0.266 (70)	−0.663 (84)	−1.437 (117)	410 (2500), 543 (6900), 918 (6800), 1380 (1400)
$Ru(PPh_3)_2(Cl_4SQ)_2$	0.897 (85)	0.539 (77)	−0.162 (82)	−0.965 (92)	440 (3600), 630 (6200), 1057 (9800), 1285 (4400)
$Ru(bpy)(Cl_4SQ)_2$[b,c]	0.94	0.57	−0.31	−1.26	420 (4140), 450 sh, 585 (10 040), 1005 (16 100), 1315 (4290)

[a] In acetonitrile (0.1 M TBAP) at 23 °C. $E_{1/2}$ = half-wave potential; ΔE = peak separation between anodic and cathodic peaks of CV. [b] Reference 5. [c] In dichoromethane.

Table VI. Selected Bond Distances and Angles for $Ru(PPh_3)_2(Cl_4SQ)_2$

Distances (Å)			
Ru–O1	1.987 (5)	C4–C5	1.422 (10)
Ru–O2	2.064 (4)	C5–C6	1.369 (10)
Ru–O3	2.053 (7)	C6–C1	1.401 (10)
Ru–O4	1.994 (5)	O3–C7	1.287 (10)
Ru–P1	2.385 (3)	O4–C8	1.312 (12)
Ru–P2	2.345 (2)	C7–C8	1.446 (13)
C1–O1	1.296 (8)	C8–C9	1.395 (12)
C2–O2	1.289 (9)	C9–C10	1.352 (17)
C1–C2	1.422 (10)	C10–C11	1.416 (16)
C2–C3	1.427 (9)	C11–C12	1.361 (14)
C3–C4	1.352 (12)	C12–C7	1.422 (15)
Angles (deg)			
P1–Ru–P2	98.9 (1)	P1–Ru–O1	90.8 (2)
P2–Ru–O1	94.7 (1)	P1–Ru–O2	87.2 (2)
P2–Ru–O2	172.1 (2)	O1–Ru–O2	80.2 (2)
P1–Ru–O3	170.0 (1)	P2–Ru–O3	90.9 (1)
O1–Ru–O3	90.0 (2)	O2–Ru–O3	83.2 (2)
P1–Ru–O4	96.9 (2)	P2–Ru–O4	92.4 (1)
O1–Ru–O4	168.6 (3)	O2–Ru–O4	91.8 (2)
O3–Ru–O4	80.9 (2)		

$(bpy)(DBSQ)_2$ given for comparison in Table V.

$Ru(PPh_3)_2(Cl_4SQ)_2$. The reaction between $Ru(PPh_3)_2(DBSQ)Cl_2$ and H_2Cl_4Cat produced two products with the minor product identified as $Ru(PPh_3)_2(Cl_4SQ)_2$. The complex was characterized crystallographically, and a view of the complex molecule is given in Figure 5. Phosphine ligands are located in cis coordination sites with one ring of each phosphine ligand paired with the π orbital of a quinone ligand. Selected bond distances and angles for the molecule are listed in Table VI. Structural features of the quinone ligands in $Ru(PPh_3)_2(Cl_4SQ)_2$ are those of semiquinones, although the increase in the number of heavy atoms in the molecule and solvent disorder have resulted in higher standard deviations for light atom distances than in the previous structure determination. The average C–O bond length is 1.296 (8) Å, and the average C–C bond length at positions that would have localized double bonds for the benzoquinone form of the ligand is 1.359 (10) Å. The electronic spectrum of $Ru(PPh_3)_2(Cl_4SQ)_2$ shown in Figure 2 is similar to that of $Ru(PPh_3)_2(DBSQ)_2$. A single low-intensity band is observed at 440 nm, and two relatively intense bands appear at 630 and 1057 nm with a distinct shoulder on the low-energy side of the 1057-nm band. Electrochemistry on $Ru(PPh_3)_2(Cl_4SQ)_2$ (Figure 4) shows two reversible reductions and two reversible oxidations. Values for the couples are shifted to positive potentials relative to the DBSQ analogue but agree well with the values reported for $Ru(bpy)(Cl_4SQ)_2$.[5]

$Ru(PPh_3)_2(DBSQ)(Cl_4SQ)$. The mixed quinone ligand complex $Ru(PPh_3)_2(DBSQ)(Cl_4SQ)$ was obtained as the major product of the reaction between $Ru(PPh_3)_2(DBSQ)Cl_2$ and H_2Cl_4Cat. ^1H NMR spectra recorded on the complex show two sets of *tert*-butyl resonances for the DBSQ ligand at 1.256–2.177 and 0.690–1.160 ppm in a ratio of 3:1, indicating the presence of two isomers. With the preference shown by the two earlier complexes for a cis disposition of phosphine ligands, the two isomers likely result from different orientations of the unsymmetrical DBSQ ligand in the cis phosphine form of the complex. Electronic spectra show the absorption at 410 nm seen in this region for the other complexes of this series, with two more intense bands at 543 and 918 nm. The low-energy transition in the near-IR region observed for the other two bis(quinone) complexes appears at 1380 nm for $Ru(PPh_3)_2(DBSQ)(Cl_4SQ)$. The infrared spectrum shown in Figure 3 contains features common to both $Ru(PPh_3)_2(DBSQ)_2$ and $Ru(PPh_3)_2(Cl_4SQ)_2$. The cyclic voltammogram of the mixed-ligand complex (Figure 4) shows the same four-couple series found for the other bis(quinone) complexes but with potentials for corresponding couples roughly intermediate between values of $Ru(PPh_3)_2(DBSQ)_2$ and $Ru(PPh_3)_2(Cl_4SQ)_2$.

Discussion

$Ru(PPh_3)_2(DBSQ)Cl_2$ has been found to be a useful precursor to both homo- and heteroligated bis(quinone) complexes. The charge distribution in $Ru(PPh_3)_2(DBSQ)Cl_2$ appears to be Ru(III)–SQ with the diamagnetism resulting from strong antiferromagnetic coupling between the paramagnetic metal and the radical semiquinone ligand. Similar coupling has been found for the related phenoxazinylate radical complex $Ru(PPh_3)_2(Phenox)Cl_2$.[11] The charge distribution in the bis(quinone) complexes $Ru(PPh_3)_2(SQ)_2$ remains as an interesting question. Lever has described the electronic structure of the $Ru(N–N)(Q)_2$ redox series in terms of a delocalized model with electronic contributions from both ligand and metal.[5] Similarities in the electronic spectra and electrochemical properties of $Ru(PPh_3)_2(SQ)_2$ and $Ru(bpy)(SQ)_2$ (SQ = DBSQ, Cl_4SQ) suggest that the complexes containing both types of counter ligands have similar electronic structures in solution. Bipyridine and phosphine ligands usually result in dramatically different electronic and electrochemical properties for complexes of ruthenium. This points to a model for electronic structure where the metal contribution to levels associated with the electronic spectra and redox activity is small and the electronic coupling between quinone ligands is strong.[6] The diamagnetism of the complexes is consistent with this model, and the smooth progression of shifts in the related redox couples for the members of the $RuL_2(DBSQ)_2$–$RuL_2(DBSQ)(Cl_4SQ)$–$RuL_2(Cl_4SQ)_2$ series is in accord with an interligand-delocalized electronic structure.

In the solid state there is a clear structural difference between the quinone ligands of the $Ru(N–N)(SQ)_2$ complexes and $Ru(PPh_3)_2(Cl_4SQ)_2$. In fact, $Ru(PPh_3)_2(Cl_4SQ)_2$ more closely resembles the oxidation product *trans*-$Ru(3\text{-}Clpy)_2(DBSQ)_2^+$ in this respect.[3] The $Ru^{III}(SQ)(Cat)$ character exhibited by the ligands of $Ru(bpy)(Q)_2$ and *trans*-$Ru(4\text{-}t\text{-}Bupy)_2(DBQ)_2$ may reflect a shift in charge distribution. This is not unprecedented for bis(semiquinone) complexes; both $Co(bpy)(DBSQ)_2$ and $Mn(py)_2(DBSQ)_2$ have different charge distributions in the solid state and in solution at room temperature.[12,13] It may further account for the weak paramagnetism of the nitrogen donor complexes in the solid state.[5]

Conclusions

In both the solid state and in solution the $Ru(PPh_3)_2(SQ)_2$ (SQ = DBSQ, Cl_4SQ) complexes have $Ru^{II}(SQ)$ charge distributions with strong electronic coupling between semiquinone ligands. The

(11) Bhattacharya, S.; Boone, S. R.; Pierpont, C. G. *J. Am. Chem. Soc.* **1990**, *112*, 4561.
(12) Buchanan, R. M.; Pierpont, C. G. *J. Am. Chem. Soc.* **1980**, *102*, 4951.
(13) Lynch, M. W.; Hendrickson, D. N.; Fitzgerald, B. J.; Pierpont, C. G. *J. Am. Chem. Soc.* **1984**, *106*, 2041.

properties of these complexes compared with the related series containing nitrogen donor ligands, $Ru(N-N)(SQ)_2$, suggest that the N-donor analogues exist as $Ru^{II}(SQ)_2$ species in solution but change in charge distribution to the $Ru^{III}(SQ)(Cat)$ form in the solid state.

Acknowledgment. This research was supported by the National Science Foundation under Grant CHE 88-09923. Ruthenium trichloride was provided by Johnson Matthey, Inc., through their Metal Loan Program. Our thanks to Prof. Arnd Vogler for providing a copy of his review article prior to publication.

Supplementary Material Available: For $Ru(PPh_3)_2(DBSQ)Cl_2$ and $Ru(PPh_3)_2(Cl_4SQ)_2$, tables giving crystal data and details of the structure determination, atom coordinates and isotropic thermal parameters, anisotropic thermal parameters, and hydrogen atom coordinates and isotropic thermal parameters (26 pages); listings of observed and calculated structure factors (32 pages). Ordering information is given on any current masthead page.

Contribution from the Anorganisch-chemisches Institut der Technischen Universität München, Lichtenbergstrasse 4, D-8046 Garching, Federal Republic of Germany

Synthesis and Structural Characterization of an Organotitanium Complex Containing a Planar Bis(μ-oxo)dititanium Core

Jun Okuda* and Eberhardt Herdtweck

Received September 25, 1990

Hydrolysis of trichloro[tris(trimethylsilyl)cyclopentadienyl]titanium, $[(\eta^5\text{-}C_5H_2(SiMe_3)_3\text{-}1,2,4]TiCl_3$ (**1**), yields with $^1/_2$ equiv of water the μ-oxo complex $[(\eta^5\text{-}C_5H_2(SiMe_3)_3\text{-}1,2,4]_2Ti_2Cl_4(\mu\text{-}O)$ (**2**), which upon further reaction with water gives dinuclear $[(\eta^5\text{-}C_5H_2(SiMe_3)_3\text{-}1,2,4]_2Ti_2Cl_2(\mu\text{-}O)_2$ (**5**). An X-ray structural determination of **5** revealed the presence of a planar $Ti_2(\mu\text{-}O)_2$ core with Ti-O distances of 1.814 (1) and 1.835 (1) Å and angles at Ti and at O of 84.23 (3) and 95.78 (3)°, respectively. The substituted cyclopentadienyl ligands are η^5-bonded and mutually trans configurated. Compound **5** crystallizes from pentane in the monoclinic space group $C2/c$, with cell dimensions a = 21.144 (1) Å, b = 9.713 (1) Å, c = 20.686 (2) Å, β = 93.90 (1)°, V = 4238 Å^3, and D(calcd) = 1.194 g·cm^{-3} (Z = 4).

Introduction

Among the transition-metal–oxo complexes bearing η^5-C_5H_5 (Cp) or η^5-C_5Me_5 (Cp*) groups as ancillary ligands,[1] titanium–oxo complexes seem to occupy a special position. While complexes featuring a terminal oxo functionality remain unknown so far,[2] a diversity of ring[3] and cage[4] frameworks in addition to the relatively common linear Ti–O–Ti core[5] have been characterized. These organotitanium complexes can be regarded as molecular models for materials formed by the extremely complicated sol–gel processes during hydrolysis of $TiCl_4$,[6] since they are usually prepared by the reaction of metallocene derivatives L_2TiX_2 or of half-sandwich complexes of the formula $LTiX_3$ (L = Cp, Cp*; X = monoanionic ligand such as halide or alkyl) with water. We report here results of our attempts to further clarify the course of these hydrolysis reactions by modifying the steric properties of the supporting cyclopentadienyl ligand and the formation of a new dinuclear organotitanoxane with a planar $Ti_2(\mu\text{-}O)_2$ core. The cyclopentadienyl ligand systems we utilized in this study are sterically highly hindered η^5-$C_5H_2(SiMe_3)_3$-1,2,4 ("Si_3Cp")[7] and η^5-$C_5H_2(CMe_3)$-4-$(SiMe_3)_2$-1,2 ("$BuSi_2Cp$").[8] They have been designed to kinetically stabilize reactive intermediates and block any bimolecular condensation reactions that would lead to high-nuclearity aggregates.[8,9]

Scheme I

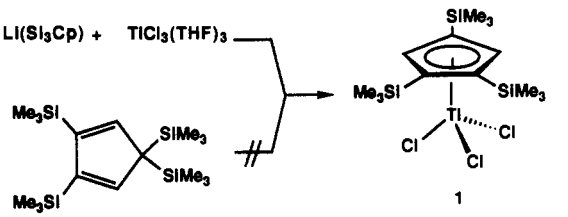

1

Results

The key compound $(Si_3Cp)TiCl_3$ (**1**), reported briefly before,[10] is accessible by reacting $TiCl_3$ or $TiCl_3(THF)_3$ with $Li(Si_3Cp)$ in THF followed by in situ oxidation of the green titanium(III) intermediate $(Si_3Cp)TiCl_2(THF)_2$. We found that carbon tetrachloride as oxidizing agent gives reproducibly $(Si_3Cp)TiCl_3$, albeit in moderate yields. The product can be isolated as pentane-soluble, orange crystals. The $BuSi_2Cp$ analogue

(1) Sutin, L.; Bottomley, F. *Adv. Organomet. Chem.* **1988**, *28*, 329.
(2) For examples without carbon ligands, see: (a) Haase, W.; Hoppe, H. *Acta Crystallogr.* **1968**, *B24*, 282. (b) Fowles, G. W. A.; Lewis, D. F.; Walton, R. A. *J. Chem. Soc. A* **1968**, 1468. (c) Guilard, R.; Lecomte, C. *Coord. Chem. Rev.* **1985**, *65*, 87. (d) Hiller, W.; Strähle, J.; Kobel, W.; Hanack, M. *Z. Kristallogr.* **1982**, *159*, 173. (e) Hill, J. E.; Fanwick, P. E.; Rothwell, I. P. *Inorg. Chem.* **1989**, *28*, 3602. (f) Recently, a reactive zirconocene–oxo complex was reported: Carney, M. J.; Walsh, P. J.; Hollander, F. J.; Bergman, R. G. *J. Am. Chem. Soc.* **1989**, *111*, 8751. Carney, M. J.; Walsh, P. J.; Bergman, R. G. *Ibid.* **1990**, *112*, 6426.
(3) (a) Gorsich, R. D. *J. Am. Chem. Soc.* **1960**, *82*, 4211. (b) Skapski, A. C.; Troughton, P. G. H. *Acta Crystallogr.* **1970**, *B26*, 716. (c) Petersen, J. L. *Inorg. Chem.* **1980**, *19*, 181. (d) Blanco, S. G.; Gomez-Sal, M. P.; Carreras, S. M.; Mena, M.; Royo, P.; Serrano, R. *J. Chem. Soc., Chem. Commun.* **1986**, 1572. (e) Gomez-Sal, M. P.; Mena, M.; Royo, P.; Serrano, R. *J. Organomet. Chem.* **1989**, *358*, 147. (f) Palacios, F.; Royo, P.; Serrano, R.; Balcazar, J. L.; Fonseca, I.; Florencio, F. *Ibid.* **1989**, *375*, 51.
(4) (a) Huffmann, J. C.; Stone, J. G.; Krusell, W. C.; Caulton, K. G. *J. Am. Chem. Soc.* **1977**, *99*, 5829. (b) Roth, A.; Floriani, C.; Chiesi-Villa, A.; Guastini, C. *Ibid.* **1986**, *108*, 6832. (c) Babcock, L. M.; Day, V. W.; Klemperer, W. G. *J. Chem. Soc., Chem. Commun.* **1987**, 858. (d) Babcock, L. M.; Klemperer, W. G. *Inorg. Chem.* **1989**, *28*, 2003.
(5) (a) Corradini, P.; Allegra, G. *J. Am. Chem. Soc.* **1959**, *81*, 5510. (b) Thewalt, U.; Schomburg, D. *J. Organomet. Chem.* **1977**, *127*, 169. (c) Thewalt, U.; Kebbel, J. *Ibid.* **1978**, *150*, 59. (d) Döppert, K. *Naturwissenschaften* **1990**, *77*, 19. (e) Gomez-Sal, M. P.; Mena, M.; Palacios, F.; Royo, P.; Serrano, R.; Carreras, S. M. *J. Organomet. Chem.* **1989**, *375*, 57.
(6) *Gmelins Handbuch der Anorganischen Chemie, Titan*; Verlag Chemie: Weinheim, FRG, 1951; p 307.
(7) Jutzi, P.; Sauer, R. *J. Organomet. Chem.* **1973**, *50*, C29.
(8) Okuda, J. *Chem. Ber.* **1989**, *122*, 1075.
(9) (a) Main group complexes: Jutzi, P. *Adv. Organomet. Chem.* **1986**, *26*, 217. (b) f-element complexes: Edelman, M. A.; Lappert, M. F.; Atwood, J. L.; Zhang, H. *Inorg. Chim. Acta* **1987**, *139*, 185. (c) Transition-metal complexes: Okuda, J. *J. Organomet. Chem.* **1987**, *333*, C41; **1988**, *353*, C1; **1989**, *367*, C1. Okuda, J.; Herdtweck, E. *Chem. Ber* **1988**, *121*, 1899. Antinolo, A.; Bristow, G. S.; Campbell, G. K.; Duff, A. W.; Hitchcock, P. B.; Kamarudin, R. A.; Lappert, M. F.; Norton, R. J.; Sarjudeen, N.; Winterborn, D. J. W. *Polyhedron* **1989**, *8*, 1601.
(10) Okuda, J. *Chem. Ber.* **1990**, *123*, 87.

0020-1669/91/1330-1516$02.50/0